LJMU Research Online

Jafer, HM, Atherton, W, Sadique, MM, Ruddock, F and Loffill, E

 Stabilisation of soft soil using binary blending of high calcium fly ash and palm oil fuel ash

http://researchonline.ljmu.ac.uk/id/eprint/7639/

Article

For more information please contact researchonline@ljmu.ac.uk

Stabilisation of Soft Soil Using Binary Blending of High Calcium Fly Ash and Palm Oil Fuel Ash

Hassnen Jafer [a,c,*], William Atherton[b], Monower Sadique[b], Felicite Ruddock[b] and Edward Loffill[b]

[a] Department of Civil Engineering, Liverpool John Moores University, Henry Cotton Building, Webster Street, Liverpool L3 2ET, UK

[b] Department of Civil Engineering, Liverpool John Moores University, Peter Jost Centre, Byrom Street, Liverpool L3 3AF, UK

[c] Department of Civil Engineering, College of Engineering, University of Babylon, Babylon, Iraq

*Corresponding author.

E-mail addresses: H.M.Jafer@2014.ljmu.ac.uk, musa_eng@yahoo.com (H. M. Jafer).

Abstract

Lime and/or Ordinary Portland cement (OPC) are the traditional binders used in soft soil stabilisation. However, their manufacture has a negative impact on the environment. This paper reports the results of experimental work for the optimisation of a binary blended cementitious binder (BBCB) using two types of fly ash as an alternative for use in soft soil stabilisation. The optimum content of the high calcium fly ash (HCFA) was initially determined along with the effect of grinding activation on the performance of HCFA. Subsequently, the effect of palm oil fuel ash (POFA) pozzolanic reactivity on the engineering properties of soft soil, stabilised with HCFA, was investigated by producing different binary mixtures of HCFA and POFA. Based on the Atterberg limits and unconfined compressive strength (UCS) tests, the combination of POFA with HCFA results in a considerably lower plasticity index (PI) and higher compressive strength than those obtained from the soil treated with HCFA alone. Substantial changes in the microstructure and binders of the stabilised soil over curing time were evidenced by SEM imaging and XRD analysis. A solid and coherent

30 structure was achieved after treatment with BBCB as evidenced by the formation of C-S-H,

31 portlandite and ettringite as well as secondary calcite.

1. Introduction

36 Soil stabilisation was technically introduced several decades ago. It is used to alter

37 undesirable soil properties, to increase shear strength and decrease compressibility, thus

38 meeting engineering specifications for project sites (Venda Oliveira *et al.*, 2011; Kalkan,

39 2013). Soft soil stabilisation has traditionally been achieved by mixing soft soils with lime,

40 cement, and/or special additives such as pozzolanic materials. Studies involving lime and

41 Ordinary Portland Cement (OPC) as preferred binder materials, report on their ability to bind

42 soil particles to each other, resulting in an improved material (Farouk and Shahien, 2013;

43 Önal, 2014; Modarres and Nosoudy, 2015). However, the manufacture of 1 tonne of OPC

44 consumes 1.5 tonnes of raw materials involving an energy consumption of 5.6 GJ/tonne and

45 CO_2 emissions of approximately 0.9 tonnes. Cement manufacture represents 6% of total

46 global CO_2 emissions, constituting a substantial environmental burden (Song and Chen,

47 2016; Zhang *et al.*, 2017). An annual growth of 6.95% has been recorded, the highest

48 increase being 9.0% in 2010 and 2011, with a slowdown to 3.0% in 2012 reaching 3.7 billion

49 tonnes. Reflecting a 5% per annum predicted increase in the global cement market

50 (Merchant Reserch & Consulting ltd, 2013), recent data for the manufacture of cement shows

51 tonnage at 4 and 4.3 billion tonnes in 2013 and 2015, respectively (CEM-Bureau, 2015).

52 Due to a negative environmental impact and the relatively high cost of cement production,

53 researchers have been motivated to create more environmentally friendly and cost-effective

54 materials to replace or reduce the use of OPC in the concrete industry. These materials are

55 generally by-products, or waste materials, most of them fly ashes (Sivrikaya *et al.*, 2014). Fly

56 ashes are most likely to have pozzolanic properties, which by themselves do not have any

57 cementitious properties, but when added to cement, react to boost the hydration process; such

58 materials are classified as class F fly ash (ASTM international, 2003; Lin *et al.*, 2007). Some

59 fly ashes have an adequate free lime content which means they exhibit high hydration

60 reactivity when mixed with water and are classified as class C fly ash. Such fly ashes have

61 been used as cement-based materials to produce new cementitious material which have been

62 used instead of OPC in numerous construction projects (Edeh *et al.*, 2014; Jafer *et al.*, 2015;

63 Dulaimi *et al.*, 2017; Jafer *et al.*, 2018).

64 Much research has been conducted using waste materials mixed with OPC or lime, to

65 produce new cementitious materials which perform better than OPC or lime alone. These

66 products have been used in a range of diverse construction projects, such as concrete for

67 building, rigid pavements and soft soil stabilisation. In such cases, these waste materials are

68 called supplementary cementitious materials (SCMs). They either have a high amorphous

69 silica content, which facilitates pozzolanic reactivity in the presence of a free lime, such as

70 palm oil fly ash (POFA), rice husk ash, pulverised fuel ash and silica fume (Kumar *et al.*,

71 2007; Jaturapitakkul *et al.*, 2011), or have a good proportion of free lime, performing as

72 cement when mixed with water, such as ground blast furnace slag, sewage sludge ash, and

73 calcium carbide residue (Fava *et al.*, 2011; Horpibulsuk *et al.*, 2012; Dave *et al.*, 2016).

74 POFA is a pozzolanic waste material produced from the palm oil industry, generated in huge

75 quantities, mainly in developing countries (Karim et al., 2013). Indonesia and Malaysia are

76 the dominant palm oil production countries, manufacturing 86% of global supplies making

77 them the premier POFA producers (Aprianti, 2017). It was reported by Shafigh et al. (2014)

78   that Malaysia's production of crude palm oil is 7 million tonnes per annum, a hundred

79   thousand tonnes of POFA per year reported to be produced by Thailand (Jaturapitakkul et al.,

80   2007). The disposal and transportation of the solid waste generated from POFA activity is

81   however a serious problem regarding both the environment and cost making it necessary to

82   address this problem, not only in terms of landfill issues but also increasing construction

83   costs and air pollution.

84   The effect of the partial replacement of cement by POFA on the compressive strength and

85   sulphate resistance of mortars was investigated by Tangchirapat et al. (2009). Compressive

86   strength with 10% POFA increased by 102% - 104% over that for OPC type I. The use of

87   ground POFA (10-40%) as a cement replacement resulted in a significant reduced rate of

88   mortar expansion in its first year of aging but the compressive strength was less than that for

89   their reference mortars. In the field of soft soil stabilisation, POFA has been used as a cement

90   replacement material in order to improve Atterberg limits and unconfined compressive

91   strength (Ahmad *et al.*, 2011; Pourakbar *et al.*, 2015). However, there are few, if any,

92   investigations of POFA as a potential pozzolanic activator with class C fly ash for use in soft

93   soil stabilisation.

94   Many researchers have utilised binary, ternary and even quaternary blending systems to

95   produce new cementitious materials from different types of waste materials and fly ashes.

96   Chemical activation methods have been used by some researchers to activate base

97   cementitious materials by adding alkaline and/or pozzolanic materials; others have applied a

98   grinding process using ball mills or mortars for mechanical activation (Antiohos *et al.*, 2007;

99   O'Rourke *et al.*, 2009; Sadique *et al.*, 2012; Dave *et al.*, 2016; Soriano *et al.*, 2016).

4

100 This study aims to improve the compressive strength of a soft soil from Hightown, near

101 Liverpool, using a binary-blended cementitious binder (BBCB) consisting of high-calcium

102 fly ash (HCFA) and POFA.

2. Materials and Methods

2.1 Soil samples

105 The soil used in this study was collected from a site located in Hightown to the north of

106 Liverpool, United Kingdom. The site is a riverbank of the River Alt estuary. The soil samples

107 were extracted from depths ranging between 30 and 50 cm below ground level. The site in

108 general is an alluvial plain; the soil is described as medium-soft, dark grey, silty clay with a

109 trace of sand.

110

111 Fig. 1 shows the particle size distribution (obtained from sieve and hydrometer analysis) of

112 the soil used in this study. It contains 13.1% sand, 43.9% silt and 43.0% clay, the main

113 physical and geotechnical properties of the soil are listed in Table 1 along with the results of

114 pH and Loss on Ignition (LOI) tests. An LOI test was performed according to British

115 standard 1377-3 (British Standard, 1999a) by adopting a procedure as explained in clause 4.

116 This test was to determine the organic matter content in the original soil, found to be equal to

117 7.95%; this value denotes that the soft soil used in this study is considered as medium organic

118 soil according to BS EN ISO 14688-2:2004+A1 (European Committee for Standardization,

119 2013). Based on BS EN ISO 14688-2:2004+A2013 (European Committee for

120 Standardization, 2013), the grain distribution and Atterberg limits (LL and PI), this soil is

121 classed as an intermediate plasticity silty clay with sand (CI).

122

123 **Fig. 1.** Particle size distribution of the silty clay.

5

124

Table 1. Physical and geotechnical properties of the silty clay.

126

2.2 Binder materials

Two different types of waste material fly ash were used in this study to produce the binary blended cementitious material:

1- High calcium fly ash (HCFA), generated from power plants using an incineration process at temperatures between 850^oC and 1100^oC by means of a fluidised bed combustion system and;

2- Palm oil fuel ash (POFA), a waste material produced from the incineration processes applied to palm oil fibres at temperatures ranging between 800 and 1000^oC, imported from the Sg. Tengi Palm Oil Factory, Kuala Kubu Bharu, Selangor, Malaysia.

2.3 Analytical techniques used for characterisation

2.3.1 Particle size distribution (PSD) of the binder materials

The PSD of the binder materials was obtained using a Laser Diffraction Particle Analyser (LDPA) brand Beckman Coulter LS 13 320. PSD curves of the fly ashes are shown in Fig. 2 alongside that of OPC for comparison purposes. It should be noted that the POFA was sieved first to remove materials which were not completely combusted using a sieve size 150μm. It was then ground with a pestle and mortar grinder for approximately 15 minutes, to increase its fineness and enhance the pozzolanic reactivity (Aprianti *et al.*, 2015). A similar procedure was adopted by Awal and Shehu (2013) for POFA preparation prior to use in experiments. From Fig. 2, it can be seen that the HCFA particles are coarser than those of OPC and POFA. This detail will affect the pozzolanic reactivity of the HCFA; this is discussed in more detail later.

148

Fig. 2. PSD of the fly ash used in this study in comparison to the PSD of OPC.

150

2.3.2 Scanning electron microscopic (SEM) analysis

This technique has been used to identify the surface morphological, particle shape and state of the raw materials used in this study along with the microstructures of the hydrated pastes of the treated soil and optimum binary mixture after being exposed for different curing periods. SEM testing was conducted using an FEI Quanta 200 scanning electron microscopy with an accelerating voltage of 10kV, however, the voltage sometimes requires adjustment to below or above 10kV to obtain better resolution. Prior to SEM imaging testing, the specimens were coated with a thin layer of palladium using a sputter coater for increased visibility. The photomicrographs of the binder materials and the virgin soil used in this study are shown in Fig. 3. The flaky-shaped particles which represent the clay in the soil are easily recognised (Fig. 3a). The HCFA particles are agglomerated and have a coagulated state occurring in clusters while POFA has spherical-shaped particles with some irregular-shaped particles with sharp angles as shown in Figs. 3b and c respectively. It was indicated by Segui *et al.* (2012) that the high porosity of binder materials with an agglomerated morphology could lead to a reduction in the workability due to the increase in the water absorbed by the large open areas of high porosity. Chandara *et al.* (2011) reported that POFA contained 67.22% of glassy phase which makes it possible to react as a pozzolanic material.

Fig. 3. SEM photomicrographs of (a) soft soil, (b) HCFA, and (c) POFA.

2.3.3 Energy dispersive X-ray fluorescence (XRF) analysis

The XRF technique was utilised to provide the elemental analysis of the binder materials used in this study along with the virgin soil. The equipment used for this technique was a

172 Shimadzu's EDX-720 Energy Dispersive X-Ray Fluorescence Spectrometer. The materials

173 were subjected to the XRF testing in their virgin dry powder state.

174 The chemical compositions of HCFA, POFA and OPC, are listed in Table 2. From this table,

175 the CaO and SiO_2 contents of HCFA are similar to those for OPC. The CaO content of the

176 HCFA used in this study is comparable to that reported by Dulaimi *et al.* (2016) (67.057%)

177 but is higher than that reported by Sadique and Al-Nageim (2012) at 57.0%. Based on the

178 chemical analysis, HCFA is promising enough to have the potential to form the basis for the

179 cementitious material as it can react with pozzolanic materials to produce cementitious

180 compounds. With respect to POFA, similar chemical properties were reported by

181 Chindaprasirt *et al.* (2014) but with slight differences, specifically in potassium and

182 aluminium oxides (Table 2).

183

184   **Table 2**. The main chemical compositions of the source materials determined by XRF.

185

186 *2.3.4 X-ray diffraction (XRD) analysis*

187 The XRD analysis was carried out using a Rigaku Miniflex diffractometer with Cu-Kα X-ray

188 radiation at a voltage of 30kV. An electrical current of 15mA was used with a scanning speed

189 of 2.0 degree/min in continuous scan mode, starting from 5° rising to 65°. The database

190 released by CDS national chemical database service was used in identifying the peaks. As

191 shown in Fig. 4a, the main mineralogical constituents of the virgin soil are quartz and

192 kaolinite while illite, calcite, potassium feldspar, plagioclase (albite phase), and muscovite

193 are the minor phases. According to Budhu (2011) and Kinuthia (2016), the minerals kaolinite,

194 illite, smectite and montmorillonite are the most common types of crystalline minerals that

195 make up clays. The powder diffraction patterns obtained from the XRD testing of the fly

8

196 ashes used in this study are shown in Figs. 4b and c. These results reveal that HCFA is

197 crystalline as it has sharp peaks without noticeable noise in the background; this can be

198 observed clearly from Fig. 4b1. The main crystals in HCFA were calcite ($CaCO_3$), lime

199 (CaO), portlandite ($Ca(OH)_2$), and gehlenite ($CaAl[AlSiO_7]$). The reflections indicated at

200 angles 2-theta of 33.3^o and 34° and 41.2^o are attributed to the presence of tricalcium

201 aluminate ($3CaO.Al_2O_3$) and belite (beta-$2CaO.SiO_2$; larnite) respectively; similar reflections

202 were reported by Gluth *et al.* (2014). Although a similar mineralogy was identified by

203 Dulaimi *et al.* (2017), in the current study, HCFA calcite intensity was found to be higher

204 than that of lime. In contrast, the dominant crystalline peaks of POFA were quartz (SiO_2),

205 while potassium aluminium phosphate ($K_3Al_2[PO_4]_3$) was identified as minor phases (Fig.

206 4c), similar to the diffraction patterns of the POFA reported by Karim *et al.* (2013). An

207 amorphicity halo has been observed in the XRD patterns of POFA in the angular 2-theta

208 range of $20 – 40^o$ as shown in Fig. 4c1. Due to the overlapping of the glassy phase of the used

209 POFA, a halo at 2-theta around 22° is shown; this indicates the existence of a glassy phase

210 and reactivity of POFA (Calligaris *et al.*, 2015).

211

212 **Fig. 4.** XRD pattern of (a) Soil, (b) HCFA, (b1) Scaled HCFA, (c) POFA and (c1) glassy
213 phase of POFA. Where: I: illite; Ka: kaolinite; Q: quartz; P: potassium feldspar; C: calcite;
214 M: muscovite; Pl: plagioclase (albite phase); CH: portlandite; G: gehlenite; L: lime; C$_3$A:
215 tricalcium aluminate; La; larnite beta-phase; and K: $K_3Al_2[PO_4]_3$.
216

217 *2.4 Sample preparation*

218 The soft soil exported from the site was first left to air-dry for a few days (not less than 4

219 days), then oven dried at 110 ± 5^oC. The soil lumps were then pulverised using a plastic

220 hammer and sieved on a sieve size 3.36mm.

221 There are two stages to the experimental work in this research. The first stage was to

222 determine the optimum percentage of HCFA to be added to the stabilised soil and the level of

223 mechanical activation (optimum time of grinding) to be used. Atterberg limits (LL, PL, and

224 PI) determination, compaction parameters (maximum dry density (MDD) and optimum

225 moisture content (OMC)) evaluation and UCS tests were utilised in the first stage. The HCFA

226 was added to the soil for these tests in six different percentages- 0, 3, 6, 9, 12 and 15% by dry

227 weight of the soil. Optimisation of the binary mixture constituted the second stage by mixing

228 POFA with HCFA as a supplementary portion of the optimum percentage of HCFA. The

229 optimum binary mixture was assessed using the UCS test. Atterberg limits and compaction

230 tests were also conducted in the second stage. Finally, and in order to understand the

231 mechanism of improvements in the strength of the stabilised soil, SEM and XRD tests were

232 conducted for the most promising mixtures after 3, 7, and 28 days of curing. Table 3

233 summarises the testing procedure adopted in this study.

234 **Table 3**. The experimental procedure for this study.

235

236 The Atterberg limits test (LL, PL and PI) for the untreated and treated soil was conducted in

237 accordance to BS 1377-2:1990 (British Standard, 1998), the LLs determined using the cone

238 penetration method. The standard Proctor test method was used to determine the compaction

239 parameters (MDD and OMC) according to BS 1377-4:1990 (British Standard, 2002).

240 With respect to the UCS test, a constant volume mould was used to prepare specimens with

241 specific dimensions (38 mm in diameter and 76 mm in height) and densities dependent on the

242 MDD and OMC obtained from the compaction test for each corresponding percentage of

243 HCFA and POFA which was added. This test was performed using a computerised and

244 motorised triaxial machine but without applying any lateral load in the triaxial cell ($\sigma_3 = 0$) in

245 accordance to BS 1377-7:1990 (British Standard, 1999b). Three specimens were prepared for

246 each corresponding percentage of the additive by compressing the soil-binder mixture inside

247 the constant volume mould using a manual hydraulic compression machine. Following this,

248 the specimens were removed from the mould, weighed, wrapped in cling film and labelled,

249 then placed in well-sealed plastic bags, stored for curing at room temperature (20 ± 2°C) for

250 3, 7, 14, and 28 days. The most promising samples were further cured up to 91 days.

251 With respect to the samples prepared for the investigation of hydration kinetics (XRD and

252 SEM analysis of the hydrated pastes), at the required curing time, fragments from inside

253 surface were taken and dried at 40°C for 12 hours to stop the hydration, the samples were

254 then subjected to the aforementioned tests without any delay. The fragments for XRD

255 analysis were ground then the powder passed through a sieve size of 150 μm was used, while

256 those for SEM testing were subjected to the procedure explained in section 2.3.2.

257

3. Results and discussion

3.1 The optimisation of HCFA content

260 Six different percentages of HCFA - 0, 3, 6, 9, 12, and 15% by dry weight, were added to the

261 soft soil in order to find the optimum percentage of HCFA, as illustrated in Table 3 above.

262 The values of MDD and OMC obtained from the compaction curves of the soil treated with

263 different percentages of HCFA are illustrated in Table 4. It is seen that the HCFA has a

264 significant effect, decreasing the MDD of the stabilised soil. In addition, the OMC increased

265 substantially with the continuous increase of HCFA. However, the results of the compaction

266 test showed that MDD decreased from 1.56 Mg/m^3 for untreated soil to 1.40 Mg/m^3 when

267 adding 15% of HCFA, while OMC increased significantly from 23% to 30.5%. This

268 behaviour is attributed to the high CaO content and the high surface area provided by HCFA,

269 which increased the water demands of the soil-binder mixture (Muhunthan and Sariosseiri,

270   2008; Jauberthie *et al.*, 2010).

271

272   **Table 4**. Compaction parameters of the soil treated with different percentages of HCFA.

273

274   Table 5 shows the Atterberg limits of the soil treated with different percentages of HCFA; LL

275   and PL increased while PI decreased significantly with an increase in HCFA content. The

276   increase in LL was due to an enlargement of the diffuse double layer (expression refers to the

277   floating cations and a few anions around clay particles) caused by an increase in the specific

278   surface area; this in turn increases the water-holding capacity of the soft soil (Das, 2010).

279   There was a constant increase in PL with the increase in HCFA content, an effect that may be

280   due to the cation exchange that occurred between the clay minerals and calcium ions (positive

281   cations) in the HCFA (Eskisar, 2015). Consequently, the PI of the treated soft soil decreased

282   in relation to the increase in HCFA content, this leading to an increase in soil workability, as

283   indicated by Baran *et al.* (2001). Similar behaviour of the Atterberg limits of a soft soil

284   treated with calcium carbide residue (CCR) was reported by Kampala and Horpibulsuk

285   (2013).

286

287   **Table 5.** The effect of HCFA on the consistency limits of the stabilised soil.

288

289   The optimum percentage of HCFA required was identified after conducting the UCS tests.

290   Fig. 5a shows the effect of HCFA on the unconfined compressive strength of the soft soil at

291   different curing periods, while Fig. 5b shows the stress-strain diagram for the soil specimens

292   at 28 days of age. The UCS was found to increase with an increase in HCFA content up to
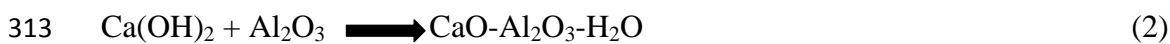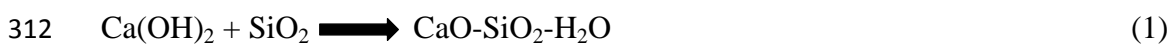
293   12%, but then decrease at 15% HCFA. The strength of the stabilised soil improved

294   significantly after the first week of curing for all percentages of HCFA. Subsequently, the

12

295 UCS increased gradually with respect to 14 and 28 days of curing, as shown in Fig. 5a. The

296 UCS test results indicated that 12% of HCFA was the optimum percentage facilitating the

297 highest values for the compressive strength of the stabilised soil across all curing times.

298

299 **Fig. 5.** (a) The relationship between the UCS and HCFA for different curing periods, and (b)

300 stress-strain diagram for undisturbed, compacted, untreated and soil treated with different

301 percentages of HCFA after 28 days' curing.

302

303 The flocculation and agglomeration phenomenon, in addition to the cation exchange that

304 occurred between the monovalent cations of the clay minerals of the stabilised soil and the

305 divalent calcium ions of the HCFA, are responsible for the early strength improvement of the

306 uncured samples (Muhunthan and Sariosseiri, 2008; James and Pandian, 2016). With

307 increases in curing time, the development in the strength of the stabilised soil occurred due to

308 the pozzolanic reaction that took place between the HCFA and the silica and the alumina of

309 the stabilised soil (Aïtcin, 2016; James and Pandian, 2016). This reaction produces cementing

310 materials including calcium-silicate-hydrate and calcium-alumina-hydrate, as shown in

311 Equations 1 and 2:

312 $Ca(OH)_2 + SiO_2 \longrightarrow CaO\text{-}SiO_2\text{-}H_2O$ (1)

313 $Ca(OH)_2 + Al_2O_3 \longrightarrow CaO\text{-}Al_2O_3\text{-}H_2O$ (2)

314

315 *3.2 Improvement for grinding of HCFA*

316 In order to explore the pozzolanic reactivity of HCFA, the optimum percentage of HCFA

317 (12%) was subjected to four different periods of grinding, namely 10, 20, 30 and 40 minutes.

318 A pestle and mortar grinder with low agitation (1 horsepower = 0.75kW) and a mortar

319 capacity of 2.5 litres was used. It has been shown that applying a grinding technique to fly

320 ash with sufficient lime content and sludge ash, enhances reactivity during hydration and

13

321 increases the formation rate of calcium-silicate hydrates (C-S-H), this resulting in improved

322 strength and setting properties (Kumar *et al.*, 2008; Zhao *et al.*, 2016). The effect of grinding

323 was established by conducting UCS tests on specimens treated with 12% of HCFA, ground

324 for different periods of time. The curves of particle size distribution shown in Fig. 6 indicated

325 that HCFA ground for only 10 minutes gave the best particle distribution. Longer periods of

326 grinding resulted in coarser grades which were closer to that for unground HCFA due to the

327 agglomeration of HCFA particles. Agglomeration occurs during intensive or longer grinding

328 periods by very strong inter-particle bonds resulting in the formation of a very compacted,

329 irreversible joining of a high number of primary particles (JuhÁSz, 1998). Moreover, the

330 dynamic force of continued grinding causes extra surface energy and surface electric charge

331 which makes the ground particles strongly subjected to attractive inter-particle forces leading

332 to the generation of aggregation and agglomeration (Sajedi and Razak, 2011; Sadique *et al.*,

333 2013).

334

335 **Fig. 6**. Effect of grinding time on particle size distribution of HCFA.

336

337 The results of the UCS tests were in strong agreement with those obtained from the PSD

338 tests, where a higher UCS value was apparent in the soil specimens treated with HCFA

339 ground for 10 minutes, as shown in Fig. 7. This is attributed to the increase in the fineness of

340 HCFA after grinding which boosts the pozzolanic reaction leading to a successful hydration

341 process and forming more cementitious products (Sanjuán *et al.*, 2015). UCS values

342 decreased as the grinding time increased beyond 10 minutes due to the agglomeration which

343 occurred, inversely affecting the pozzolanic reactivity of HCFA and disrupting the hydration

344 process (Sadique *et al.*, 2012; Sadique *et al.*, 2013). Table 6 illustrates the development of

345 UCS over curing time for both the untreated soil and the soil treated with 12% of normal and

14

346 ground HCFA (Table 3, U4 and GU respectively). The soil treated with activated HCFA

347 achieved higher UCS values over the curing periods. By 28 days of age, UCS had increased

348 by 112.5% after the application of grinding. It should be noted that 12% HCFA was then

349 used as the total binder content for the remaining experimental work in this study.

350 It was shown that the mechanical activation of additive materials using the grinding

351 technique was successful, leading to an increase in the specific surface area and the

352 production of finer materials which, in turn, enhanced the pozzolanic reactivity of the

353 supplementary cementitious materials (SCMs). Increasing the fineness of binder materials

354 boosts the hydration process increasing the production of cementitious gel, which in turn

355 increases compressive strength (Sanjuán *et al.*, 2015; Velandia *et al.*, 2016). .

356

357 **Fig. 7**. Effect of grinding time on UCS for specimens with 12% HCFA at 7 days of age.

358

359 **Table 6.** Effect of grinding activation (GU) on the development of UCS over curing time.

360

361 *3.3 Optimisation for the binary mixtures*

362 The optimum binary mixture was identified from the UCS tests conducted on soil specimens

363 treated with 12% of different mixtures of HCFA+POFA, as indicted in Table 3. The effect of

364 binary blending on compaction parameters and consistency limits was also explored in this

365 study. The portions of HCFA used in the binary mixtures were mechanically activated by 10

366 minutes of grinding, as explained in Table 7. The results for the compaction parameters of the

367 soil treated with the binary blending of HCFA and POFA, are also illustrated in Table 7. It

368 can be seen that MDD increased and OMC decreased gradually with the increase in

369 percentage of POFA. As per the chemical composition of POFA, this fly ash has less CaO

370 content in comparison to that found in HCFA. Thus, the increase in POFA content in the

15

371 binary mixture decreases the water demand of the binder produced which, in turn, increases

372 the MDD and decreases the OMC. This agrees with studies conducted using fly ash type F in

373 contrast with studies using fly ash type C, which has a higher CaO content (Harichane *et al.*,

374 2011; Sivrikaya *et al.*, 2014) .

375 **Table 7.** Effect of binary blending on compaction parameters of stabilised soil.

376

377 The consistency limits of the soil treated with 12% normal and ground HCFA (Table 3, U4

378 and GU) and different binary mixtures are listed in Table 8. Binary blending is very effective

379 in decreasing the PI of stabilised soil; said PI decreased in parallel with a continuous increase

380 of POFA content in the binary mixture. From Table 8 it can be seen that an increase in the

381 amount of POFA, as a replacement for HCFA in the binary mixture, produces decreases in

382 both LL and PL, the decrease in LL greater than that for PL; PI also then decreases. The

383 decrease in LL and PL is attributed to the decrease in water demand due to a reduction in

384 HCFA from 12% (GU) in the binary mixture as shown in Table 3.

385

386 **Table 8**. Effect of grinding and binary blending on Atterberg limits of the stabilised soil.

387

388 Unconfined compressive strength testing was conducted on soil specimens treated with

389 different binary mixtures in order to identify the optimum combination. The specimens were

390 tested after curing periods of 3, 7, 14, and 28 days, the most promising mixtures exposed to a

391 prolonged curing period of 91 days to determine the compressive strength under long term

392 curing. Fig. 8 shows the effect of binary blending on the UCS of the treated soil in

393 comparison to the UCS of the soil treated with HCFA alone at different curing periods. These

394 results indicated that HCFA failed to exhibit substantial pozzolanic reaction in either of its

395 unary mixture states (U4 and GU) when compared with the binders containing POFA, while

16

396 considerable improvement in UCS was observed with all the binary mixtures. It can be

397 concluded from Fig. 8 that the optimum mixture was BM2, produced by mixing 9% HCFA

398 with 3% POFA by dry weight of the stabilised soil. BM1 and BM3 gave similar results,

399 specifically in the early curing periods.

400

401 **Fig. 8**. UCS development for different mixtures and curing periods.

402

403 Over a prolonged curing time (91 days), the UCS of the stabilised soil with mixtures U4, GU

404 and BM2 had significant improvements of 111.16%, 112% and 114.61%, respectively, in

405 comparison to their values at 28 days of curing. The successful development of UCS using

406 binary blending is due to the high pH of both fly ashes used in this study, along with the silica

407 component provided mainly from the glass phase of POFA. The glass phase of silica

408 components dissolves quickly in the alkaline conditions which in turn boosts the chemical

409 activation of HCFA. This leads to a successful hydration reaction, transforming the calcium

410 hydroxide of HCFA into calcium silicate hydrate (C-S-H). Pourakbar *et al.* (2015) reported a

411 similar significant improvement in the UCS of the soil by using 10% binder of binary mixture

412 containing cement-to-POFA proportion of 80:20.

413

3.4 The kinetics of optimum binary mixture hydration

415 Fig. 9 shows the phase composition of the dry powder state of BBCB and the comparative

416 diffraction patterns of its hydrated paste at different curing periods. Clear differences can be

417 distinguished in the dry state of the XRD peaks for BBCB and the individual dry states of

418 both types of fly ash. However, the intensities of various peaks are dependent on the

419 participating percentage of each type of fly ash in the binary mixture. In terms of the hydrated

420 states, the amorphous structure of C-S-H and C-A-S-H gels makes it very difficult for them to

17

be identified by XRD (Sadique *et al.*, 2012); such types of hydrates would be reflected in hump forms around 2 theta values 29.5^o, 32° and 50° as reported by Kulasuriya *et al.* (2014). However, peaks of different carbonates and hydrates can be distinguished since the early age of hydration (three days) such as calcite ($CaCO_3$), portlandite ($Ca(OH)_2$) and ettringite ($Ca_6Al_2 (SO_4)_3 (OH)_{12}. 26H_2O$). At this age of hydration, the peaks of C3A and larnite (<beta>-C2S) that indicated in the dry powder state of BBCB (non-hydrated) were no longer exist after hydration due to their high reactivity. These compounds were expected to provide the required calcium, silica and alumina along with the silica produced from the dissolution of the glassy phase of POFA to form the C-S-H and C-A-H gel (Gluth *et al.*, 2014). With the progress of curing time, the peak intensities of portlandite decreased and then approximately disappeared while some of ettringite peaks and C-S-H became more pronounced, specifically after 28 days. A progression in the intensities of calcite peaks was also observed due to CO_2 effect on portlandite from air in wet conditions. XRD analysis also revealed a broad peak at 3 days of curing around the angle 2-theta 11.1^o suggests the presence of a semi-amorphous C-A-H which became more likely as an amorphous gel after 28 days. A similar finding was reported by Rajamma *et al.* (2009) after XRD analysis of a paste prepared from cement replaced by 30% fly ash. A peak of monocarboaluminate hydrate ($Ca_4Al_2O_6.CO_3.11H_2O$); CO_3-AFm was observed after 7 days of curing at 2-theta 11.7^o which developed to be more pronounced after 28 days of hydration. This compound is formed by the chemical reaction between the ettringite and C3A due to the AlO_2^- diffusion which is expected to continue in release even after the sulphate being used up (Peng *et al.*, 2006). The generation of C-S-H gel and CH is attributed to the chemical reaction occurring between the lime (L) and amorphous silica provided by HCFA and POFA, respectively. These compounds are expected to be formed continuously as curing time progresses because the pozzolanic reaction of silica requires a longer period to activate HCFA to form more C-S-H gel (Calligaris *et al.*, 2015;

18

446 Jiang *et al.*, 2016). The XRD results show that at the early stages of curing, some peaks of

447 CH developed then decreased at 28 days curing. This indicates that CH was activated with

448 the pozzolanic materials provided by POFA and transformed to C-S-H compounds. Similar

449 findings were reported by Sadique *et al.* (2013) after using a calcium-rich fly ash activated by

450 a high alkali sulphate fly ash.

451

452 **Fig. 9**. XRD patterns of BM2 (BBCB) in dry and hydrated states with different curing
453 periods (CH: portlandite, C-S-H: calcium silicate hydrate; C-A-H: calcium aluminate
454 hydrate; E: ettringite; Q: quartz; L: lime; La: larnite; C: calcite; C_3A: tricalcium aluminate;
455 and Mc: monocarboaluminate hydrate).

456

457 The consequent changes in the microstructure of the BBCB pastes, with and without soil, due

458 to hydration over different curing periods, 3, 7, and 28 days, are shown in the SEM test

459 images, Figs. 10a-f respectively. These changes were very clear and represented by the

460 formation of flaky shaped CH crystals and C-S-H gel in addition to needle-shaped crystals

461 (ettringite) which occurred due to the hydration reaction. Ettringite was initially observed at

462 an earlier hydration stage (3 days) with a small amount of CH crystals, as shown in Figs. 10a

463 and d, the subsequent formation of ettringite and CH continuing becoming denser at 7 days

464 curing. At this age, the SEM images showed that some particles of the soil (Fig. 10b) and

465 particles of BBCB (Fig. 10e) were coated with C-S-H gel. Regarding longer curing periods

466 (28 days), uniform and larger amounts of cementitious products were observed, represented

467 by the transformation of most of the CH crystals to C-S-H gel as shown in Figs. 10c and f.

468 Additionally, the rhombohedral structure of calcite crystals was observed clearly in the

469 BBCB paste after 28 days of curing as illustrated in Fig. 10f. The high alkalinity of HCFA

470 and POFA enhanced the dissolution of the glassy phases of HCFA and POFA and produced

471 additional C-S-H gel. This gel tends to fill pores and grow into capillary spaces, resulting in a

472 more impermeable, dense and higher-strength structure (Blanco *et al.*, 2006; Kulasuriya *et*

473 *al.*, 2014).

474 When the gypsum source becomes entirely consumed and the C3A continue to dissolve and

475 provide more ions of Ca^{2+} and AlO_2^-, the ettringite starts to react with the newly produced

476 ions and transforms into AFm phase (Marchon and Flatt, 2016). However, longer curing and

477 associated hydration reactions within an alkaline environment were expected to cover the

478 ettringite with a thick layer of C-S-H gel which prevents the diffusion of AlO_2^- and disrupts

479 its reaction with ettringite (Peng *et al.*, 2006).

480

481 **Fig. 10**. SEM images of hydrated pastes of (a) to (c) soil-BBCB and (d) to (f) BM2 (BBCB).

482

483 **4. Conclusions**

484 The effect of the mechanical activation using low intensity grinding of HCFA, along with the

485 effect of pozzolanic activation using POFA, were analysed in this paper. This provides a

486 novel approach for the use of waste materials in the development of a new binder for use in

487 soft soil stabilisation. According to the results, the following conclusions can be drawn:

488 • Despite the HCFA having a chemical composition similar to that of OPC, it has less

489 potential as pozzolanic activator than OPC. However, the HCFA has much free lime as

490 well as a small amount of glassy phase. Therefore, it is beneficial to produce a BBCB

491 mixed HCFA with high glassy POFA in order to produce high performance pozzolanic

492 cement for the use in soft soil stabilisation.

493 • Due to the high water demands of HCFA, MDD decreased and OMC increased with an

494 increase in HCFA content. However, the results of the compaction parameter test

495 indicated slight increments in MDD and reductions in OMC with the use of POFA.

20

496   These increments in density contributed to improvements in the strength of the stabilised

497   soil.

498 • HCFA was found to be very effective in improving the consistency limits of the

499   stabilised soil, where the PI decreased from 20.2 for the untreated soil, to 13.38 by using

500   12% mechanically activated HCFA. No significant effect was observed using POFA in

501   the binary mixtures, but the PI continued to decrease, dropping to 11.73 for the soil

502   treated with BM4. This reduction in PI will substantially improve the resistance of

503   stabilised soil against swelling and shrinkage stresses.

504 • Mechanical activation using grinding energy activated the pozzolanic reaction of HCFA

505   by increasing the surface area. However, the results of mechanical activation indicated

506   that long periods of grinding led to agglomeration which caused a reduction in

507   compressive strength due to the decrease in pozzolanic reactivity. Mixing a de-

508   agglomeration material with HCFA during the grinding process would mitigate the effect

509   of extended periods of grinding.

510 • The results of the UCS tests indicate that the optimum BBCB (BM2) mixture comprises

511   HCFA and POFA at a ratio of 9:3. The performance of this mixture as a binder in soft

512   soil stabilisation was very promising in that soil strength improved significantly from

513   200 kPa for untreated soil to 1059 kPa for the soil treated with 12% of BBCB at age 90

514   days; this improvement is 5.7 times the UCS for compacted virgin soil.

515 • The XRD patterns of the BBCB hydrated paste revealed clear changes in peak intensities

516   over curing time. This explains the consumption of some of BBCB compounds, such as

517   lime and portlandite during the hydration processes, resulting in the formation of new

518   compounds e.g. C-S-H and ettringite in addition to the calcite resulted from the CH

519   carbonation. It may be concluded that the latter compounds contributed to the

520   development of the strength of the soil stabilised with BBCB.

- SEM images for BBCB hydrated paste provided evidence to support the XRD analysis. A sequent formation of C-S-H, CH, calcite and ettringite was observed, over time of curing, using SEM testing which confirms the cementitious property of the BBCB. A similar behaviour was observed in the cured soil-BBCB pastes, a stronger soil structure achieved at 28 days curing.

Acknowledgements

References

Ahmad, J.,Abdul Rahman, A. S.,Mohd Ali, M. R. & Abd. Rahman, K. F. 2011. Peat soil treatment using pofa. *IEEE Colloquium on Humanities, Science and Engineering Research.* Malaysia, Penang.

Aïtcin, P. C. 2016. 4 - supplementary cementitious materials and blended cements. *Science and technology of concrete admixtures.* Woodhead Publishing. Available: http://www.sciencedirect.com/science/article/pii/B9780081006931000047

Antiohos, S. K.,Papadakis, V. G.,Chaniotakis, E. & Tsimas, S. 2007. Improving the performance of ternary blended cements by mixing different types of fly ashes. *Cement and Concrete Research,* 37**,** 877-885.

Aprianti, E. 2017. A huge number of artificial waste material can be supplementary cementitious material (scm) for concrete production – a review part ii. *Journal of Cleaner Production,* 142**,** 4178-4194.

Aprianti, E.,Shafigh, P.,Bahri, S. & Farahani, J. N. 2015. Supplementary cementitious materials origin from agricultural wastes – a review. *Construction and Building Materials,* 74**,** 176-187.

22

546 ASTM international 2003. Standard specification for coal fly ash and raw or calcined natural pozzolan

547   for use in concrete. *C 618 – 03*. USA: ASTM international.

548 Awal, A. S. M. A. & Shehu, I. A. 2013. Evaluation of heat of hydration of concrete containing high

549   volume palm oil fuel ash. *Fuel,* 105**,** 728-731.

550 Baran, B.,Ertu̇rk, T.,Sarıkaya, Y. & Alemdaroğlu, T. 2001. Workability test method for metals

551   applied to examine a workability measure (plastic limit) for clays. *Applied Clay Science,* 20**,** 53 -

552   63.

553 Blanco, F.,Garcia, M. P.,Ayala, J.,Mayoral, G. & Garcia, M. A. 2006. The effect of mechanically and

554   chemically activated fly ashes on mortar properties. *Fuel,* 85**,** 2018-2026.

555 British Standard 1998. Bs 1377-2, methods of test for soils for civil engineering purposes - part 2:

556   Classification tests. london: UK: British Standard Institution.

557 British Standard 1999a. Bs 1377-3, methods of test for soils for civil engineering purposes — part 3:

558   Chemical and electro-chemical tests. London, UK: British Standard.

559 British Standard 1999b. Bs 1377-7, methods of test for soils for civil engineering purposes - part 7:

560   Shear strength tests (total stress). London: UK: British Standard istitute

561 British Standard 2002. Bs 1377-4, methods of test for soils for civil engineering purposes - part4:

562   Compaction-related tests. London: UK: British Standard institut.

563 Budhu, M. 2011. *Soil mechanics and foundations,* United States of America, JOHN WILEY &

564   SONS, INC.

565 Calligaris, G. A.,Franco, M. K. K. D.,Aldrige, L. P.,Rodrigues, M. S.,Beraldo, A. L.,Yokaichiya,

566   F.,Turrillas, X. & Cardoso, L. P. 2015. Assessing the pozzolanic activity of cements with added

567   sugar cane straw ash by synchrotron x-ray diffraction and rietveld analysis. *Construction and*

568   *Building Materials,* 98**,** 44-50.

569 CEM-Bureau. 2015. *Key fact & figures* [Online]. The European Cement Association. Available:

570   http://www.cembureau.be/about-cement/key-facts-figures [Accessed 19-08-2016 2016].

571 Chandara, C.,Azizli, K. A. M.,Ahmed, Z. A.,Hashim, S. F. S. & Sakai, E. 2011. Analysis of

572   mineralogical component of palm oil fuel ash with or without unburned carbon. *Advanced*

573   *Materials Research,* 173**,** 7 - 11.

574 Chindaprasirt, P.,Sinsiri, T.,Kroehong, W. & Jaturapitakkul, C. 2014. Role of filler effect and
575   pozzolanic reaction of biomass ashes on hydrated phase and pore size distribution of blended
576   cement paste. *Journal of Materials in Civil Engineering,* 26**,** 04014057.

577 Das, B. M. 2010. *Principles of geotechnical engineering,* United States of America, CENGAGE
578   Learning.

579 Dave, N.,Misra, A. K.,Srivastava, A. & Kaushik, S. K. 2016. Experimental analysis of strength and
580   durability properties of quaternary cement binder and mortar. *Construction and Building*
581   *Materials,* 107**,** 117-124.

582 Dulaimi, A.,Al Nageim, H.,Ruddock, F. & Seton, L. 2016. New developments with cold asphalt
583   concrete binder course mixtures containing binary blended cementitious filler (bbcf). *Construction*
584   *and Building Materials,* 124**,** 414-423.

585 Dulaimi, A.,Al Nageim, H.,Ruddock, F. & Seton, L. 2017. High performance cold asphalt concrete
586   mixture for binder course using alkali-activated binary blended cementitious filler. *Construction*
587   *and Building Materials,* 141**,** 160-170.

588 Edeh, J. E.,Agbede, I. O. & Tyoyila, A. 2014. Evaluation of sawdust ash–stabilized lateritic soil as
589   highway pavement material. *Journal of Materials in Civil Engineering,* 26**,** 367 - 373.

590 Eskisar, T. 2015. Influence of cement treatment on unconfined compressive strength and
591   compressibility of lean clay with medium plasticity. *Arabian Journal for Science and Engineering,*
592   40**,** 763-772.

593 European Committee for Standardization 2013. Bs en iso 14688-2:2004+a2013. Geotechnical
594   investigation and testing - identification and classification of soil, part 2: Principles for a
595   classification. London: UK: British Standard Institution.

596 Farouk, A. & Shahien, M. M. 2013. Ground improvement using soil–cement columns: Experimental
597   investigation. *Alexandria Engineering Journal,* 52**,** 733-740.

598 Fava, G.,Ruello, M. L. & Corinaldesi, V. 2011. Paper mill sludge ash as supplementary cementitious
599   material. *Journal of Materials in Civil Engineering,* 23**,** 772-776.

600 Gluth, G. J. G.,Lehmann, C.,Rübner, K. & Kühne, H.-C. 2014. Reaction products and strength

601 development of wastepaper sludge ash and the influence of alkalis. *Cement and Concrete*

602 *Composites,* 45**,** 82-88.

603 Harichane, K.,Ghrici, M. & Kenai, S. 2011. Effect of curing time on shear strength of cohesive soils

604 stabilized with combination of lime and natural pozzolana. *International Journal of Civil*

605 *Engineering,* 9**,** 90 - 96.

606 Horpibulsuk, S.,Phetchuay, C. & Chinkulkijniwat, A. 2012. Soil stabilization by calcium carbide

607 residue and fly ash. *Journal of Materials in Civil Engineering,* 24**,** 184-193.

608 Jafer, H. M.,Atherton, W. & Ruddock, F. M. 2015. Soft soil stabilisation using high calcium waste

609 material fly ash. *12th International Post-Graduate Research Conference 2015.* Manchister

610 MediaCityUK

611 Jafer, H. M.,Atherton, W.,Sadique, M.,Ruddock, F. & Loffill, E. 2018. Development of a new ternary

612 blended cementitious binder produced from waste materials for use in soft soil stabilisation.

613 *Journal of Cleaner Production,* 172**,** 516-528.

614 James, J. & Pandian, P. K. 2016. Industrial wastes as auxiliary additives to cement/lime stabilization

615 of soils. *Advances in Civil Engineering,* 2016**,** 1-17.

616 Jaturapitakkul, C.,Kiattikomol, K.,Tangchirapat, W. & Saeting, T. 2007. Evaluation of the sulfate

617 resistance of concrete containing palm oil fuel ash. *Construction and Building Materials,* 21**,** 1399-

618 1405.

619 Jaturapitakkul, C.,Tangpagasit, J.,Songmue, S. & Kiattikomol, K. 2011. Filler effect and pozzolanic

620 reaction of ground palm oil fuel ash. *Construction and Building Materials,* 25**,** 4287-4293.

621 Jauberthie, R.,Rendell, F.,Rangeard, D. & Molez, L. 2010. Stabilisation of estuarine silt with lime

622 and/or cement. *Applied Clay Science,* 50**,** 395-400.

623 Jiang, J.,Lu, Z.,Niu, Y.,Li, J. & Zhang, Y. 2016. Investigation of the properties of high-porosity

624 cement foams based on ternary portland cement–metakaolin–silica fume blends. *Construction and*

625 *Building Materials,* 107**,** 181-190.

626 JuhÁSz, Z. A. 1998. Colloid-chemical aspects of mechanical activation. *Particulate Science and*

627 *Technology,* 16**,** 145-161.

25

628 Kalkan, E. 2013. Preparation of scrap tire rubber fiber–silica fume mixtures for modification of clayey

629 soils. *Applied Clay Science,* 80-81**,** 117-125.

630 Kampala, A. & Horpibulsuk, S. 2013. Engineering properties of silty clay stabilized with calcium

631 carbide residue. *Journal of Materials in Civil Engineering,* 25**,** 632-644.

632 Karim, M. R.,Zain, M. F. M.,Jamil, M. & Lai, F. C. 2013. Fabrication of a non-cement binder using

633 slag, palm oil fuel ash and rice husk ash with sodium hydroxide. *Construction and Building*

634 *Materials,* 49**,** 894-902.

635 Kinuthia, J. M. 2016. Unfired clay materials and construction.

636 Kulasuriya, C.,Vimonsatit, V.,Dias, W. P. S. & Silva, P. D. 2014. Design and development of alkali

637 pozzolan cement (apc). *Construction and Building Materials,* 68**,** 426-433.

638 Kumar, A.,Walia, B. S. & Bajaj, A. 2007. Influence of fly ash, lime, and polyester fibers on

639 compaction and strength properties of expansive soil. *JOURNAL OF MATERIALS IN CIVIL*

640 *ENGINEERING,* 19**,** 242–248.

641 Kumar, S.,Kumar, R.,Bandopadhyay, A.,Alex, T. C.,Ravi Kumar, B.,Das, S. K. & Mehrotra, S. P.

642 2008. Mechanical activation of granulated blast furnace slag and its effect on the properties and

643 structure of portland slag cement. *Cement and Concrete Composites,* 30**,** 679-685.

644 Lin, D.-F.,Lin, K.-L. & Luo, H.-L. 2007. A comparison between sludge ash and fly ash on the

645 improvement in soft soil. *Journal of the Air & Waste Management Association,* 57**,** 59-64.

646 Marchon, D. & Flatt, R. J. 2016. 8 - mechanisms of cement hydration. *Science and technology of*

647 *concrete admixtures.* Woodhead Publishing. Available:

648 http://www.sciencedirect.com/science/article/pii/B9780081006931000084

649 Merchant Reserch & Consulting ltd. 2013. *World cement production increased by around 3% in 2012*

650 [Online]. Available: http://mcgroup.co.uk/news/20130802/cement-production-increased-3.html

651 [Accessed 19th January 2015 2015].

652 Modarres, A. & Nosoudy, Y. M. 2015. Clay stabilization using coal waste and lime — technical and

653 environmental impacts. *Applied Clay Science,* 116-117**,** 281-288.

654 Muhunthan, B. & Sariosseiri, F. 2008. Interpretation of geotechnical properties of cement treated

655 soils. Washington State University Department of Civil & Environmental Engineering.

26

656   O'Rourke, B.,McNally, C. & Richardson, M. G. 2009. Development of calcium sulfate–ggbs–

657   portland cement binders. *Construction and Building Materials,* 23**,** 340-346.

658   Önal, O. 2014. Lime stabilization of soils underlying a salt evaporation pond: A laboratory study.

659   *Marine Georesources & Geotechnology,* 33**,** 391-402.

660   Peng, J.,Zhang, J. & Qu, J. 2006. The mechanism of the formation and transformation of ettringite.

661   *Journal of Wuhan University of Technology - Mater. Sci. Ed.,* 21**,** 158 - 161.

662   Pourakbar, S.,Asadi, A.,Huat, B. B. K. & Fasihnikoutalab, M. H. 2015. Stabilization of clayey soil

663   using ultrafine palm oil fuel ash (pofa) and cement. *Transportation Geotechnics,* 3**,** 24-35.

664   Rajamma, R.,Ball, R. J.,Tarelho, L. A.,Allen, G. C.,Labrincha, J. A. & Ferreira, V. M. 2009.

665   Characterisation and use of biomass fly ash in cement-based materials. *J Hazard Mater,* 172**,**

666   1049-60.

667   Sadique, M. & Al-Nageim, H. 2012. Hydration kinetics of a low carbon cementitious material

668   produced by physico-chemical activation of high calcium fly ash. *Journal of Advanced Concrete*

669   *Technology,* 10**,** 254-263.

670   Sadique, M.,Al-Nageim, H.,Atherton, W.,Seton, L. & Dempster, N. 2013. Mechano-chemical

671   activation of high-ca fly ash by cement free blending and gypsum aided grinding. *Construction*

672   *and Building Materials,* 43**,** 480-489.

673   Sadique, M.,Al Nageim, H.,Atherton, W.,Seton, L. & Dempster, N. 2012. A new composite

674   cementitious material for construction. *Construction and Building Materials,* 35**,** 846-855.

675   Sajedi, F. & Razak, H. A. 2011. Effects of thermal and mechanical activation methods on

676   compressive strength of ordinary portland cement–slag mortar. *Materials & Design,* 32**,** 984-995.

677   Sanjuán, M. Á.,Argiz, C.,Gálvez, J. C. & Moragues, A. 2015. Effect of silica fume fineness on the

678   improvement of portland cement strength performance. *Construction and Building Materials,* 96**,**

679   55-64.

680   Segui, P.,Aubert, J. E.,Husson, B. & Measson, M. 2012. Characterization of wastepaper sludge ash

681   for its valorization as a component of hydraulic binders. *Applied Clay Science,* 57**,** 79-85.

682   Shafigh, P.,Mahmud, H. B.,Jumaat, M. Z. & Zargar, M. 2014. Agricultural wastes as aggregate in

683   concrete mixtures – a review. *Construction and Building Materials,* 53**,** 110-117.

27

684 Sivrikaya, O.,Kıyıldı, K. R. & Karaca, Z. 2014. Recycling waste from natural stone processing plants

685   to stabilise clayey soil. *Environmental Earth Sciences,* 71**,** 4397-4407.

686 Song, D. & Chen, B. 2016. Extended exergy accounting for energy consumption and co2 emissions of

687   cement industry—a basic framework. *Energy Procedia,* 88**,** 305-308.

688 Soriano, L.,Payá, J.,Monzó, J.,Borrachero, M. V. & Tashima, M. M. 2016. High strength mortars

689   using ordinary portland cement–fly ash–fluid catalytic cracking catalyst residue ternary system

690   (opc/fa/fcc). *Construction and Building Materials,* 106**,** 228-235.

691 Tangchirapat, W.,Jaturapitakkul, C. & Kiattikomol, K. 2009. Compressive strength and expansion of

692   blended cement mortar containing palm oil fuel ash. *Journal of Materials in Civil Engineering,* 21**,**

693   426-431.

694 Velandia, D. F.,Lynsdale, C. J.,Provis, J. L.,Ramirez, F. & Gomez, A. C. 2016. Evaluation of

695   activated high volume fly ash systems using na2so4, lime and quicklime in mortars with high loss

696   on ignition fly ashes. *Construction and Building Materials,* 128**,** 248-255.

697 Venda Oliveira, P. J.,Correia, A. A. S. & Garcia, M. R. 2011. Effect of organic matter content and

698   curing conditions on the creep behavior of an artificially stabilized soil. *JOURNAL OF*

699   *MATERIALS IN CIVIL ENGINEERING,* 24**,** 868–875.

700 Zhang, X.,Shen, J.,Wang, Y.,Qi, Y.,Liao, W.,Shui, W.,Li, L.,Qi, H. & Yu, X. 2017. An environmental

701   sustainability assessment of china's cement industry based on emergy. *Ecological Indicators,* 72**,**

702   452-458.

703 Zhao, J.,Wang, D.,Yan, P.,Zhao, S. & Zhang, D. 2016. Particle characteristics and hydration activity

704   of ground granulated blast furnace slag powder containing industrial crude glycerol-based grinding

705   aids. *Construction and Building Materials,* 104**,** 134-141.

706

HIGHLIGHTS

1. A cement-free binder has been developed for soft soil stabilisation.

2. HCFA significantly contributed to the development of geotechnical properties.

3. The role of grinding, used to activate the pozzolanic reactivity of HCFA, was examined.

4. POFA's pozzolanic reactivity vigorously activated the HCFA.

5. USC development was evidenced through the use of SEM and XRD techniques.

List of abbreviations:

BBCB: binary blended cementitious binder.

HCFA: high calcium fly ash.

LDPA: Laser Diffraction Particle Analyser.

LOI: loss on ignition.

MDD: maximum dry density.

OMC: optimum moisture content.

OPC: Ordinary Portland cement.

POFA: palm oil fuel ash.

PSD: particle size distribution.

SCMs: supplementary cementitious materials.

SEM: scanning electron microscopy.

UCS: unconfined compressive strength.

XRD: X-ray diffraction.

XRF: X-ray fluorescence.

Table 1: Physical and geotechnical properties of the silty clay.

Property	Value
Natural Moisture Content NMC %	36.8
Liquid Limit LL %	44
Plastic Limit PL %	23.8
Plasticity index PI	20.2
Sand %	13.1
Silt %	43.9
Clay %	43
Specific Gravity (Gs)	2.57
γ_{dmax} Mg/m^3	1.57
Optimum moisture content OMC %	23
pH	7.78
Organic Matter Content %	7.95
Unconfined Compressive Strength for undisturbed soil (kPa)	66.46

Mg/m^3= Mega gram/cubic metre.

Table 2
Click here to download Table: Table 2.docx

Table 2. The main chemical compositions of the source materials determined by XRF.

Item	Soft soil	OPC	HCFA	POFA
CaO %	4.485	66.119	66.760	9.047
SiO_2 %	59.884	24.909	25.120	53.011
Al_2O_3 %	7.334	1.728	2.380	6.487
Fe_2O_3 %	3.850	1.668	0.030	4.873
MgO %	2.856	1.322	2.570	1.329
P_2O_5	0.096	-	-	1.794
Na_2O %	1.337	1.357	1.718	1.496
K_2O %	2.960	0.836	0.310	6.501
SO_3 %	0.343	2.655	0.380	2.531

Table 3. The experimental procedure for this study.

Mixture ID	Binder added (%) by dry weight of the stabilised soil		The experiments conducted on the binder-stabilised soil					
	HCFA	POFA	LL	PL	Compaction	UCS	SEM	XRD
UN	0	0	*	*	*	*	*	*
U1	3	0	*	*	*	*	NR	NR
U2	6	0	*	*	*	*	NR	NR
U3	9	0	*	*	*	*	NR	NR
U4	12	0	*	*	*	*	NR	NR
U5	15	0	*	*	*	*	NR	NR
GU	12% ground activated	0	*	*	NR	*	NR	NR
BM1	10.5	1.5	NR	NR	*	*	NR	NR
BM2	9	3	*	*	*	*	*	*
BM3	7.5	4.5	NR	NR	*	*	NR	NR
BM4	6	6	*	*	*	*	NR	NR

UN: refers to the untreated soft soil; U: from unary mixture; GU: for the ground unary mixture; BM: for binary mixture; *: for the conducted experiments; and NR: is not required.

Table 4. Compaction parameters of the soil treated with different percentages of HCFA.

HCFA %	MDD (Mg/m^3)	OMC %
0 (UN)	1.56	23.0
3	1.48	26.0
6	1.46	27.5
9	1.45	28.0
12	1.44	29.0
15	1.40	30.5

Table 5. The effect of HCFA on the consistency limits of the stabilised soil.

HCFA %	LL (%)	PL (%)	PI
0 (UN)	44.0	23.8	20.2
3	47.0	30.4	16.6
6	49.2	34.9	14.3
9	50.5	36.5	14.0
12	51.3	37.8	13.5
15	52.5	39.4	13.1

Table 6. Effect of grinding activation (GU) on the development of UCS over curing time.

Mix. ID	UCS (kPa) at different curing periods (days)			
	Uncured	7	14	28
(UN)	202	206	210	231
U4	367	570	642	690
GU	360	622	725	776

Table 7. Effect of binary blending on compaction parameters of stabilised soil.

Normal HCFA %	Ground HCFA %	POFA %	Mixture ID	MDD (Mg/m^3)	OMC %
0.00	0.00	0.00	Virgin soil	1.56	23.50
12.00	0.00	0.00	U4	1.44	29.00
-	12.00	0.00	GU	1.43	30.00
-	10.50	1.50	BM1	1.45	27.50
-	9.00	3.00	BM2	1.46	26.50
-	7.50	4.50	BM3	1.47	25.50
-	6.00	6.00	BM4	1.48	24.50

Table 8. Effect of grinding and binary blending on Atterberg limits of the stabilised soil.

Mix. ID	LL (%)	PL (%)	PI
UN	44.0	23.8	20.2
U4	51.3	37.8	13.5
GU	52.2	38.8	13.4
BM1	51.4	38.3	13.1
BM2	49.3	36.5	12.8
BM4	48.6	36.5	12.1
BM5	48.0	36.3	11.7
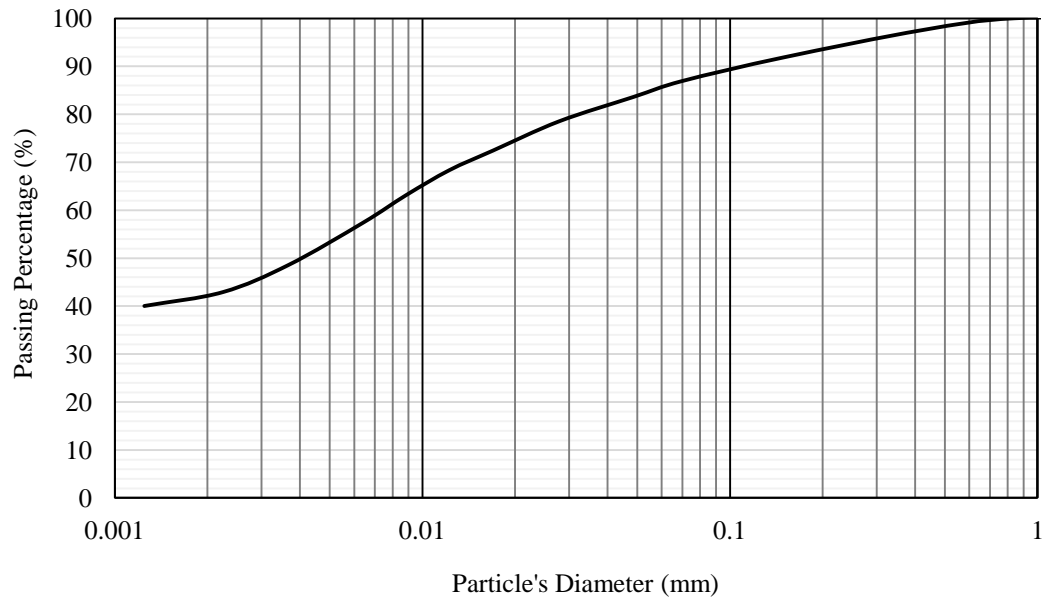
Fig. 1. Particle size distribution of the silty clay.

Figure 2
Click here to download Figure: Fig. 2.docx
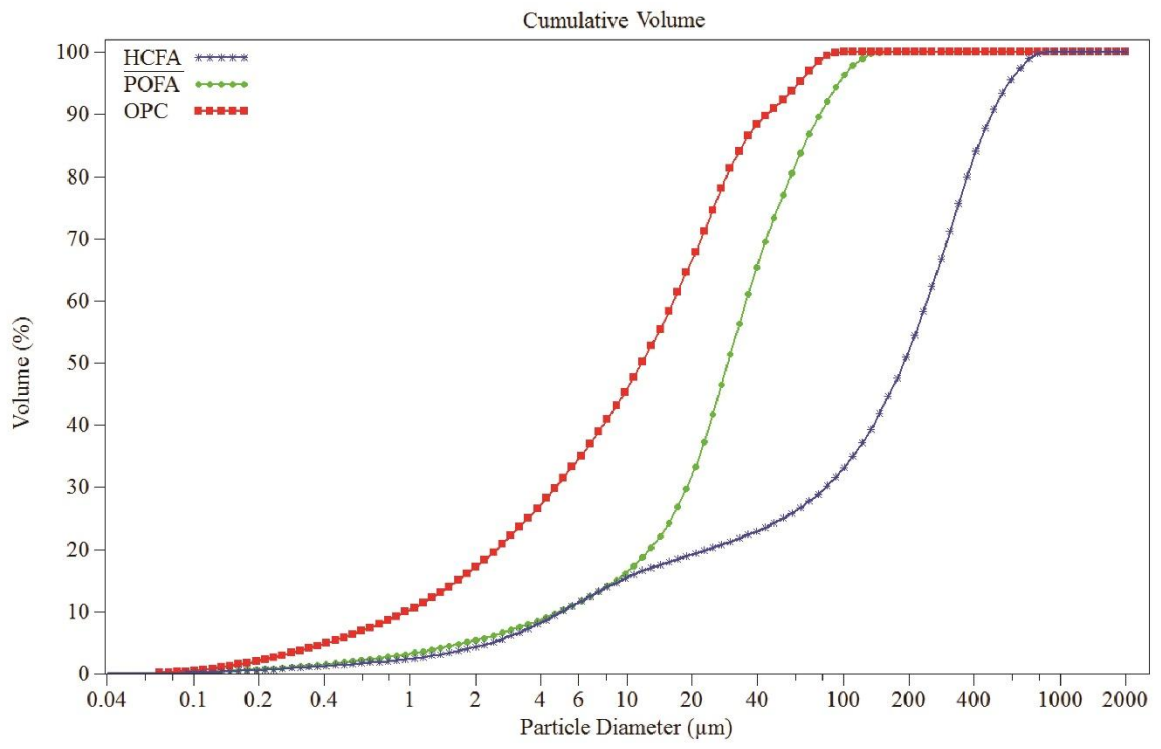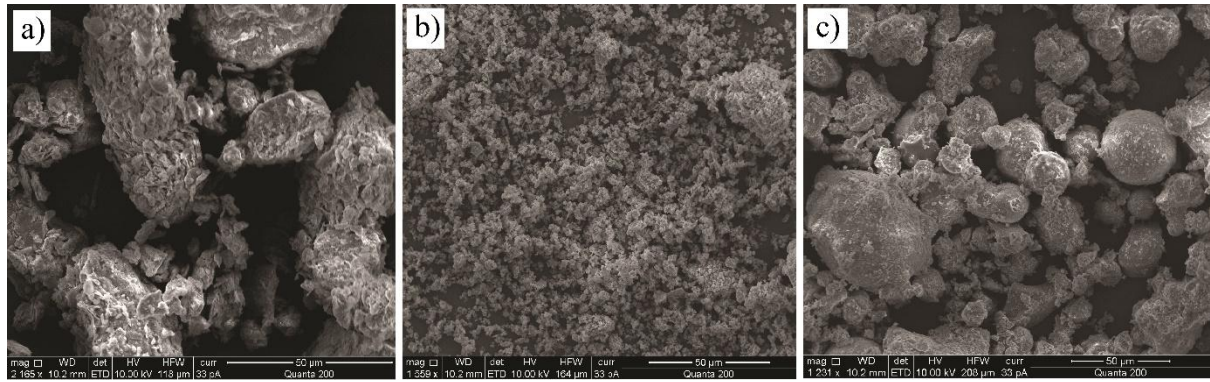
Fig. 2. PSD of the fly ash used in this study in comparison to the PSD of OPC.

Fig. 3. SEM photomicrographs of (a) soft soil, (b) HCFA, and (c) POFA.
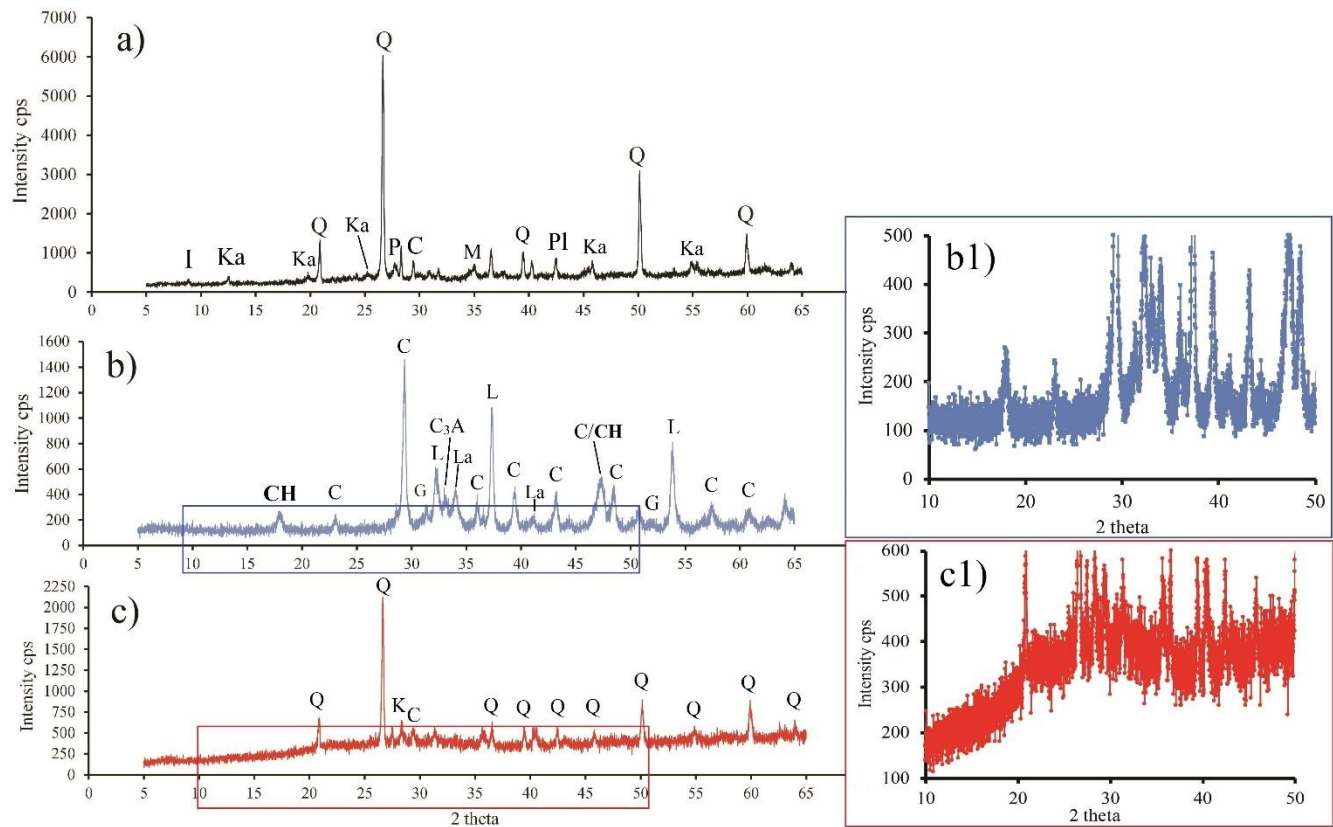
Fig. 4. XRD pattern of (a) Soil, (b) HCFA, (b1) Scaled HCFA, (c) POFA and (c1) glassy phase of POFA. Where: I: illite; Ka: kaolinite; Q: quartz; P: potassium feldspar; C: calcite; M: muscovite; Pl: plagioclase (albite phase); CH: portlandite; G: gehlenite; L: lime; C_3A: tricalcium aluminate; La; larnite beta-phase; and K: $K_3Al_2[PO_4]_3$.

Figure 5
Click here to download Figure: Fig. 5.docx
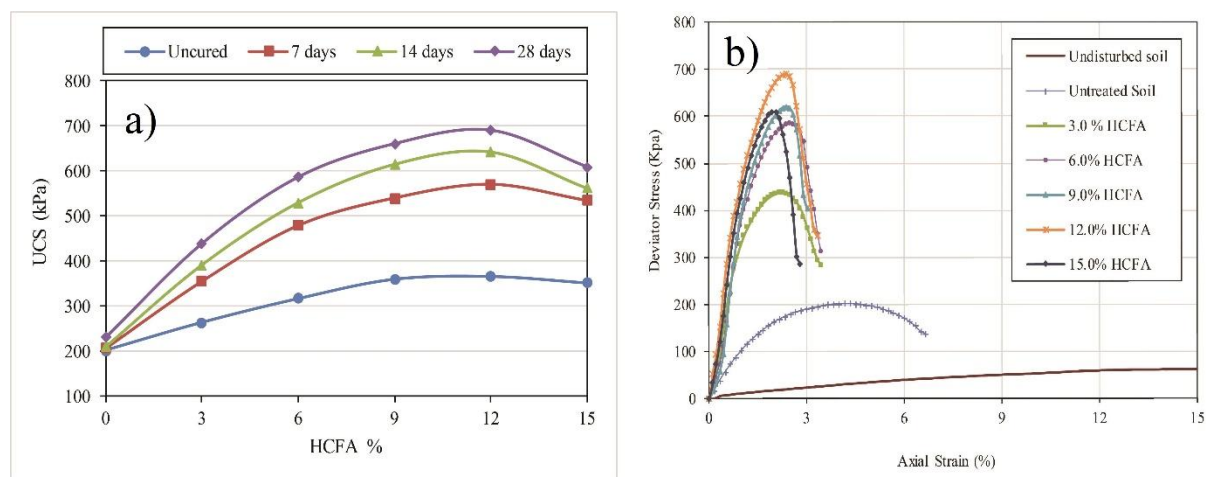
Fig. 5. (a) The relationship between the UCS and HCFA for different curing periods, and (b) stress-strain diagram for undisturbed, compacted, untreated and soil treated with different percentages of HCFA after 28 days' curing.

Figure 6
Click here to download Figure: Fig. 6.docx
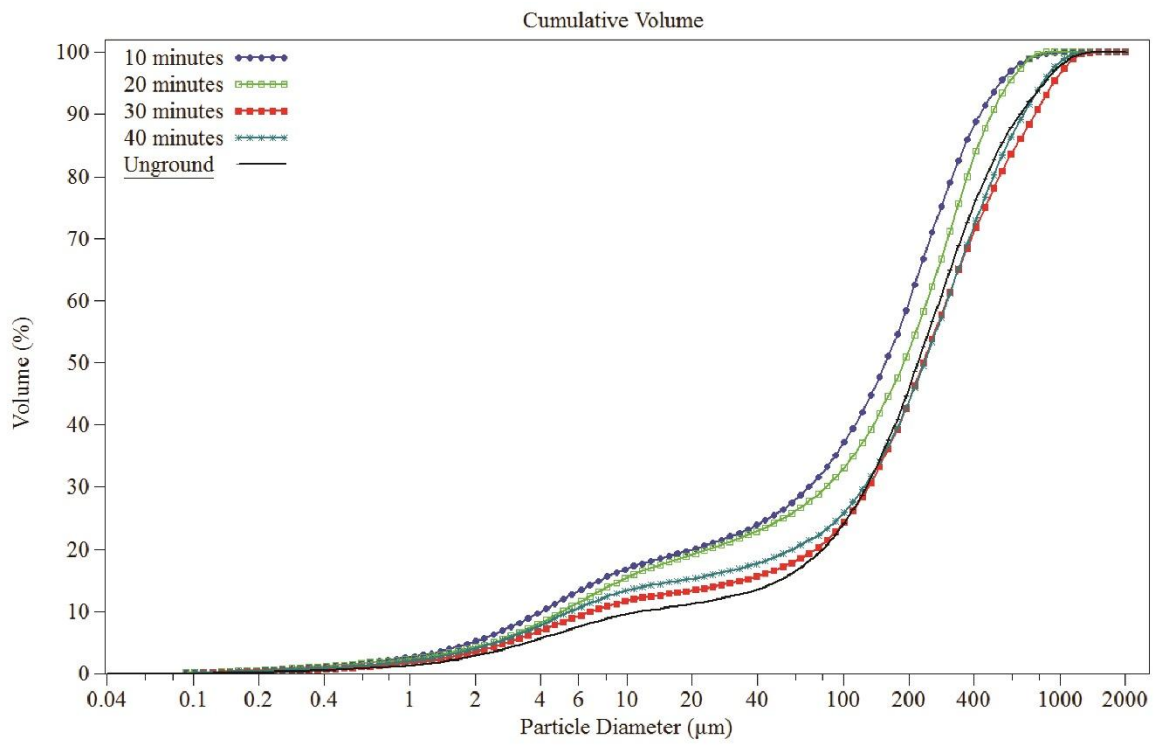
Fig. 6. Effect of grinding time on particle size distribution of HCFA.

Figure 7
Click here to download Figure: Fig. 7.docx
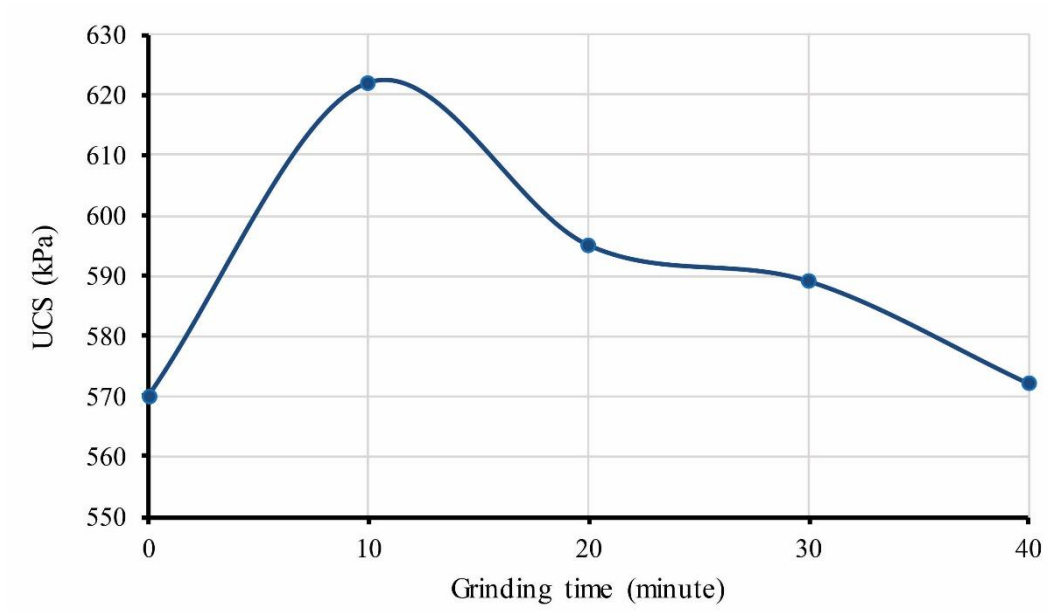
Fig. 7. Effect of grinding time on UCS for specimens with 12% HCFA at 7 days of age.
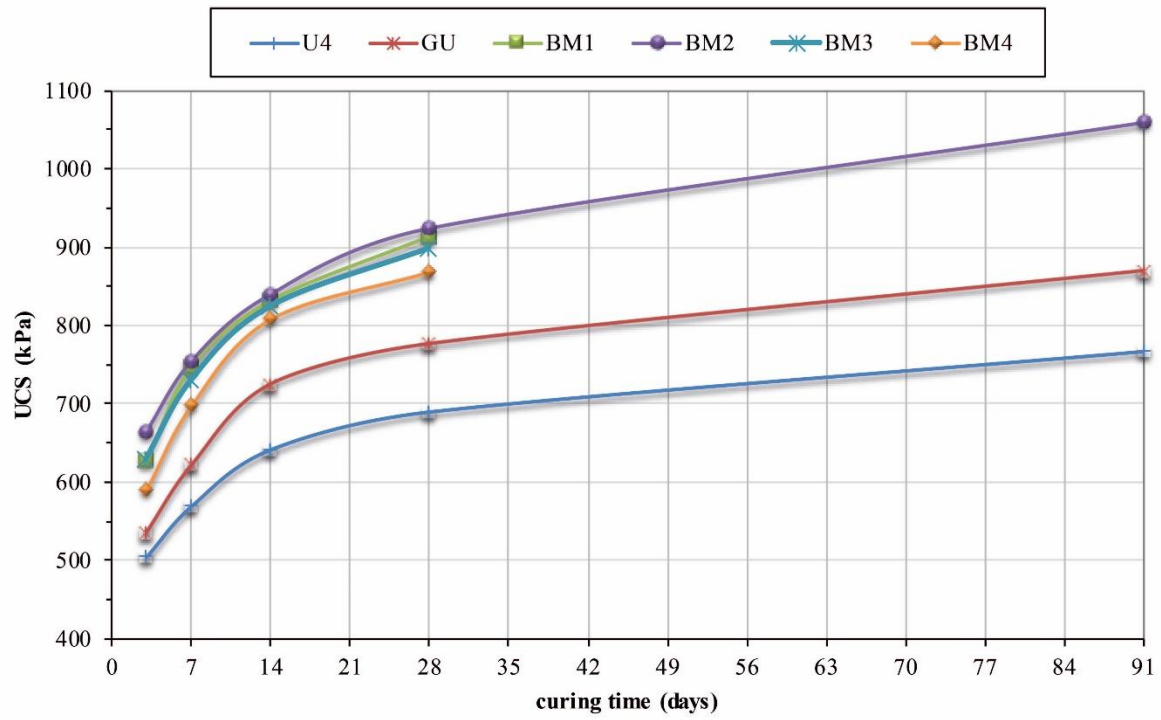
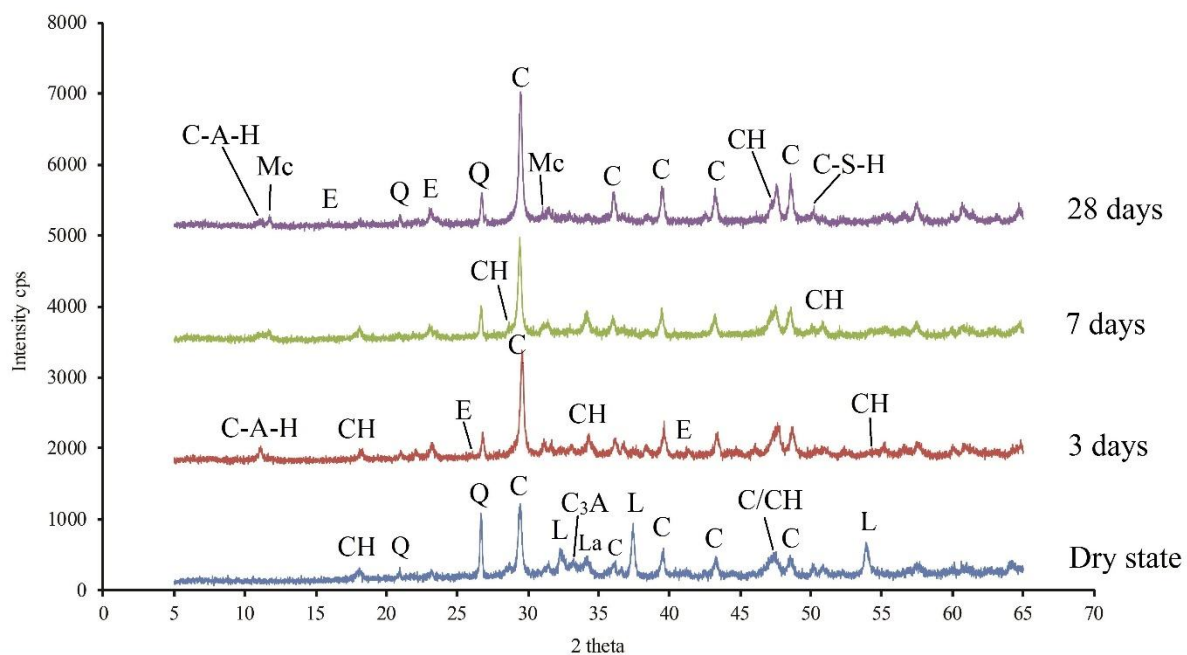**Fig. 8**. UCS development for different mixtures and curing periods.

Fig. 9. XRD patterns of BM2 (BBCB) in dry and hydrated states with different curing periods (CH: portlandite, C-S-H: calcium silicate hydrate; C-A-H: calcium aluminate hydrate; E: ettringite; Q: quartz; L: lime; La: larnite; C: calcite; C_3A: tricalcium aluminate; and Mc: monocarboaluminate hydrate).
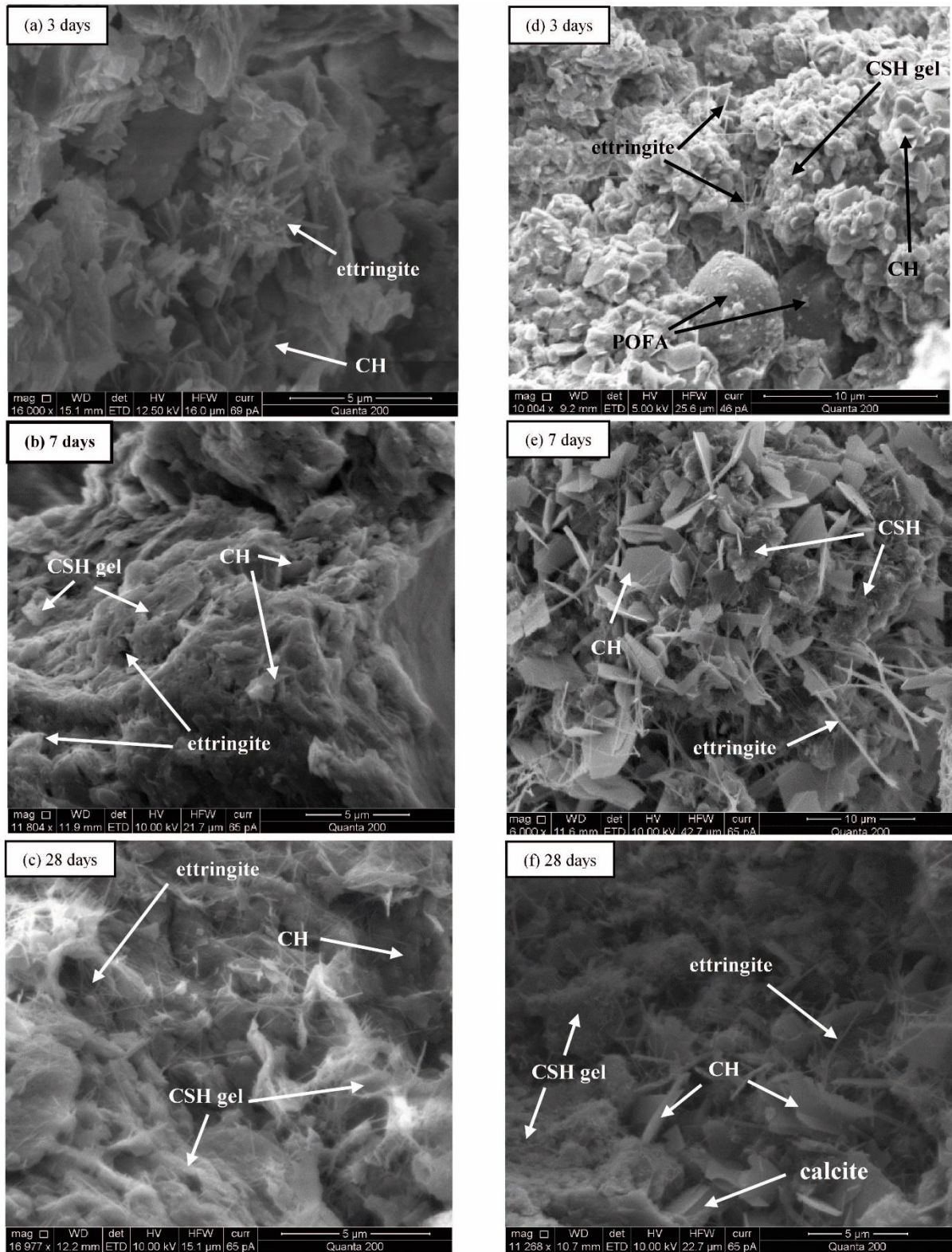
Fig. 10. SEM images of hydrated pastes of (a) to (c) soil-BBCB and (d) to (f) BM2 (BBCB).